Discovery of Chile Niño/Niña

Article *in* Geophysical Research Letters · February 2020

DOI: 10.1029/2019GL086468

4 authors, including:

Jing-Jia Luo
Japan Agency for Marine-Earth Science Technology
86 PUBLICATIONS **6,829** CITATIONS
SEE PROFILE

Chaoxia Yuan
Nanjing University of Information Science & Technology
20 PUBLICATIONS **201** CITATIONS
SEE PROFILE

Toshio Yamagata
Japan Agency for Marine-Earth Science Technology
380 PUBLICATIONS **28,534** CITATIONS
SEE PROFILE

Geophysical Research Letters

RESEARCH LETTER
10.1029/2019GL086468

Discovery of Chile Niño/Niña

Jiaqing Xue[1], Jing-Jia Luo[1], Chaoxia Yuan[1,2], and Toshio Yamagata[1,2]

[1]Key Laboratory of Meteorological Disaster of Ministry of Education, Joint International Research Laboratory of Climate and Environment Change, Collaborative Innovation Center on Forecast and Evaluation of Meteorological Disasters, Institute for Climate and Application Research (ICAR), Nanjing University of Information Science and Technology, Nanjing, China, [2]Application Laboratory, Japan Agency for Marine-Earth Science and Technology, Yokohama, Japan

Key Points:
- A new intrinsic climate mode is discovered off the coast of northern Chile and named Chile Niño/Niña for the first time
- The coastal Bjerknes feedback involving the ocean-atmosphere-land interaction plays an essential role in generating Chile Niño/Niña
- The anomalous shortwave radiation by a stratus cloud feedback and variation of the mixed-layer depth influence Chile Niño/Niña evolution

Supporting Information:
- Supporting Information S1

Correspondence to:
J.-J. Luo and T. Yamagata,
jjluo@nuist.edu.cn;
yamagata@jamstec.go.jp

Citation:
Xue, J., Luo, J.-J., Yuan, C., & Yamagata, T. (2020). Discovery of Chile Niño/Niña. *Geophysical Research Letters*, *47*, e2019GL086468. https://doi.org/10.1029/2019GL086468

Received 28 NOV 2019
Accepted 13 FEB 2020
Accepted article online 18 FEB 2020

Abstract A new air-sea coupled mode is discovered off the coast of northern Chile and named Chile Niño/Niña. It shows remarkable interannual variability in sea surface temperature (SST) with the peak in austral summer from January to March. The related warm (cold) SST anomalies are mainly generated by anomalous southward (northward) alongshore surface winds that suppress (enhance) the coastal upwelling and subsurface mixing and, in turn, reinforce the wind anomalies by heating (cooling) the overlying atmosphere and strengthening the anomalous cross-shore pressure contrast. The positive feedback is called the coastal Bjerknes feedback in analogy to the equatorial Bjerknes feedback that is responsible for generation of El Niño–Southern Oscillation. The anomalous surface shortwave radiation through the SST-low stratus cloud thermodynamic feedback and the variation in the mixed-layer depth play positive roles in the evolution of Chile Niño (Niña). In contrast, the wind-evaporation-SST feedback plays almost no role in the evolution.

Plain Language Summary The coastal air-sea coupled modes occur along eastern boundaries of most of major subtropical oceans and have noticeable biogeochemical impacts on marine ecosystems. However, no such phenomenon has been reported in the southeast Pacific so far. Here, by carefully removing the influence of El Niño–Southern Oscillation, we have discovered a new coastal climate mode off northern Chile and named it Chile Niño/Niña. The intrinsic climate mode along the coast is generated by the coastal Bjerknes feedback among alongshore surface winds, coastal upwelling, and the SST anomalies. The anomalous surface shortwave radiation and the variation in the mixed-layer depth contribute to the evolution of Chile Niño/Niña. Our results reveal the existence and generation mechanism of Chile Niño/Niña for the first time, which advance our knowledge of ocean-atmosphere-land coupled interactions and may provide new insights into the research of marine ecology and blue economy.

1. Introduction

Active ocean-atmosphere coupling over equatorial oceans generates several important climate modes, such as the El Niño–Southern Oscillation (ENSO; Bjerknes, 1969; Philander, 1990), Indian Ocean Dipole (IOD; Saji et al., 1999; Webster et al., 1999), and the Atlantic Niño (Zebiak, 1993), which contribute remarkably to the interannual variability of tropical sea surface temperatures (SSTs). Among those, ENSO is the strongest one; it is known to be generated by the equatorial Bjerknes feedback between trade winds and SST anomalies through oceanic processes (Bjerknes, 1969; Philander et al., 1984). To some degree, coastal oceans off the eastern boundaries of subtropical basins are dynamically analogous to equatorial oceans, because equatorward alongshore surface winds drive subsurface cold water upwelling just like the equatorial upwelling driven by the trade winds (Yoshida, 1959). Anomalous alongshore surface winds induce coastal SST anomalies through upwelling processes, and the resultant SST anomalies in turn force the atmosphere and influence the land-sea pressure gradient, thus reinforcing initial alongshore wind anomalies. The regional positive feedback involving the ocean-atmosphere-land interaction is called the coastal Bjerknes feedback (Kataoka et al., 2014; Yuan & Yamagata, 2014), through which anomalous SST warming/cooling events occur in eastern boundary of subtropical basins interannually. Those El Niño/La Niña-like phenomena are named coastal Niño/Niña in analogy of ENSO.

Since those coastal regions correspond to habitats of highly productive but also fragile marine ecosystems, the occurrence of coastal Niño/Niña events thus have critical impacts on marine ecology and blue

economy (Binet et al., 2001; Capone & Hutchins, 2013; Prospectus for CLIVAR Research Focus on Eastern Boundary Upwelling Systems, 2018). For example, an extreme Ningaloo Niño off the west coast of Australia in the southeast Indian Ocean in 2011 severely damaged local fishery and coral reef (Depczynski et al., 2013; Pearce & Feng, 2013; Wernberg et al., 2013). Therefore, investigating the occurrence and underlying drivers of coastal Niño/Niña are of great biological and socioeconomic importance.

In previous studies, several coastal Niño/Niña phenomena have been identified and catalogued as coastal climate modes. Those are the well-known Benguela Niño/Niña off southwestern Africa (Lübbecke et al., 2010; Shannon et al., 1986), Ningaloo Niño/Niña off western Australia (Feng et al., 2013; Kataoka et al., 2014, 2017; Tozuka et al., 2014), California Niño/Niña off the west coast of North America (Durazo & Baumgartner, 2002; Simpson, 1983; Yuan & Yamagata, 2014), and the Dakar Niño/Niña off Senegal (Oettli et al., 2016). Those climate modes are located at regions with active coastal upwelling and along the eastern rims of subtropical highs. In fact, the coastal oceans off Chile are also characterized by strong upwelling all year round (Figure S1 in the supporting information). Moreover, the SST anomalies there are found to exhibit strong interannual variability. For example, an extreme warm SST event occurred during March 2015, causing catastrophic floods over Chile's Atacama Desert and extremely warm surface air temperature throughout Southern Chile (Barrett et al., 2016; Wilcox et al., 2016). Hence, it is reasonable to expect a similar coastal phenomenon even in the South Pacific. However, we cannot find such a clear signal off the west coast of subtropical South America (Figure S2a). This may be due to the influence of strong ENSO variability on the north side including the recently emphasized *coastal El Niño*, which represents stand-alone SST variability off Peru in the far-eastern Pacific (Hu et al., 2019; Lübbecke et al., 2019; Takahashi & Martínez, 2019). Therefore, identifying coastal Niño/Niña in the subtropical South Pacific is a challenge, and this motivates us to do the present research.

2. Data and Methodology

2.1. Data Sets

The SST data used is the Hadley Centre SST (HadISST) with 1° × 1° resolution during 1958–2013 (Rayner et al., 2003). Monthly mean atmospheric reanalysis data for the same period, including sea level pressure, surface winds (10 m), air temperature, geopotential height, and low cloud cover are obtained from the Japanese 55-year Reanalysis (JRA-55), the longest third generation reanalysis that assimilates the full observing systems (Kobayashi et al., 2015). From the same data set, the sensible and latent heat fluxes, as well as surface net shortwave and longwave radiation are employed to investigate atmosphere-ocean heat exchanges. All surface heat flux components are positive downward. The ocean subsurface temperature and horizontal circulation are based on the Simple Ocean Data Assimilation (SODA) version 2.2.4 spanning 1958–2010 (Carton & Giese, 2008). Moreover, the climatology of ocean vertical velocity is provided by Global Ocean Data Assimilation System (GODAS) data over 1982–2013 (Behringer & Xue, 2004).

2.2. Methods

The mixed-layer depth (MLD) is defined as the depth where ocean temperature decreases from the near-surface value at 10 m by 0.2 °C (de Boyer Montégut et al., 2004). On this basis, mixed-layer heat balance is diagnosed by taking MLD variation into account. Following Kataoka et al. (2017), the mixed-layer temperature tendency equation is expressed as follows:

$$\frac{\partial T_m}{\partial t} = \frac{Q}{\rho c_p h} - \frac{1}{h}\int_{-h}^{0} \mathbf{V}\cdot\nabla_h T dz - \frac{1}{h}\int_{-h}^{0} \nabla_h\cdot(\kappa_h \nabla_h T) dz + \frac{q_{-h}}{\rho c_p h} \quad (1)$$

where T_m is the mixed-layer mean temperature, Q is net surface heat flux into the ocean, and ρ and c_p are the density and specific heat of sea water, respectively. h is the MLD; $\mathbf{V}$ is the horizontal velocity; κ_h is horizontal diffusion coefficient; q_{-h} denotes heat flux at the bottom of the mixed-layer representing entrainment, which, in turn, can be influenced by vertical advection (Greatbatch, 1985). The four terms on the right-hand side of equation (1) represent surface heating/cooling, horizontal advection, horizontal diffusion, and vertical processes, respectively. Because of the smallness of horizontal diffusion, the fourth term can thus be estimated by the difference between the mixed-layer temperature tendency and the first two terms on the right-hand side (Kataoka et al., 2017; Morioka et al., 2011; Morioka et al., 2012).

To better understand anomalous surface heating/cooling term, its variation can be written as follows:

$$\left(\frac{Q}{\rho c_p h}\right)' = \frac{Q'}{\rho c_p \overline{h}} - \frac{\overline{Q}}{\rho c_p \overline{h}}\frac{h'}{\overline{h}} + \mathrm{Res}, \tag{2}$$

where the overbar (prime) here indicates the long-term climatology (anomaly). The first term on the right is associated with surface heat flux anomaly and called the flux anomaly effect; the second term is contributed by climatological surface heat flux under changing mixed layer heat capacity and thus referred to as the heat capacity anomaly effect. The residual represents higher-order nonlinear terms (Kataoka et al., 2017; Morioka et al., 2010).

Since both alongshore winds induced Ekman transport and wind stress curl induced Ekman pumping drive upwelling, the coastal upwelling index is thus defined by summing the offshore Ekman transport and vertical transport due to Ekman pumping over the coastal region (Castelao & Barth, 2006; Fennel et al., 2012; Pickett & Paduan, 2003; Santos et al., 2012). The calculation is based on the JRA55 wind fields over 80°–70°W and 35°–20°S (see supporting information Text S1 for more details). Moreover, the alongshore wind index and MLD index are constructed by averaging meridional surface winds and MLD over the same region, respectively. To represent ENSO signal, especially the SST variability associated with coastal El Niño in the far-eastern Pacific, the Niño1 + 2 index is thus employed, which is defined as the areal averaged SST anomalies over the region 90°–80°W and 10°S–0°.

3. Results

3.1. The Identification of Chile Niño/Niña

It is natural to consider that the subtropical SST variability off the west coast of South America is dominated by nearby ENSO signal spreading from the tropics (Figure S2a). However, careful analyses demonstrate the SST anomalies off Chile include those independent of ENSO (Figure S2b). Here we show the warm event in 1960 and the cold event in 1991 as two examples. The off-Chile SST warm/cold events are found to occur without preceding or simultaneous ENSO signal, suggesting the existence of drivers other than ENSO (Figures S3 and S4). To investigate the intrinsic SST variability linked to subtropical air-sea interaction, the simultaneous ENSO signal represented by Niño1 + 2 index is then removed from the interannually varying monthly mean SST for each month of the year by linear regression. The standard deviation of the residual SST anomalies shown in Figure 1a now captures the striking SST variations off the west coast of Chile. The first empirical orthogonal function (EOF) mode of the SST anomalies displays a similar pattern to the standard deviation and explains 45% of the total variances (Figure 1b). Hereafter, we call this coastal phenomenon "Chile Niño/Niña". Based on the EOF analysis, the Chile Niño/Niña index (CNI) is defined simply as the mean residual SST anomalies (with the ENSO signal removed) over the domain extending from 80°W to 70°W and from 35°S to 20°S (blue box in Figure 1a). As expected, the monthly CNI is highly consistent with the principle component of EOF1 with a correlation of 0.82, which is significant at the 99% confidence level (Figure 1c). Hence, the CNI captures well the coastal SST variability off Chile. Figure 1d shows the seasonally stratified standard deviation of CNI. We find that the evolution of Chile Niño/Niña is phase locked to the annual cycle, with the largest interannual variability in austral summer from January to March (JFM), just like Ningaloo Niño/Niña, when the coastal MLD is the shallowest (Figure S5). On this basis, the general seasonal evolution of Chile Niño is presented in Figure S6. No preceding or simultaneous ENSO signal is found to accompany the Chile Niño, suggesting it is a new concrete climate signal independent of ENSO.

3.2. Air-sea Coupled Variations Linked to Chile Niño/Niña

The coevolutions of atmospheric circulation and SST anomalies are derived by calculating lead-lag regressions onto the JFM CNI. As depicted in Figure 2, low sea level pressure anomalies and associated cyclonic anomalies are observed off Chile 2–3 months prior to the peak of Chile Niño. This atmospheric precursor may be related to the variability of the South Pacific High. The anomalous cyclone corresponds to southward alongshore surface wind anomalies, which lead to the weakening of offshore Ekman transport and coastal upwelling, thus contributing to the warming of SST. Once the coastal ocean is anomalously warmed through oceanic processes, it starts heating the overlying atmosphere and induces baroclinic responses over the

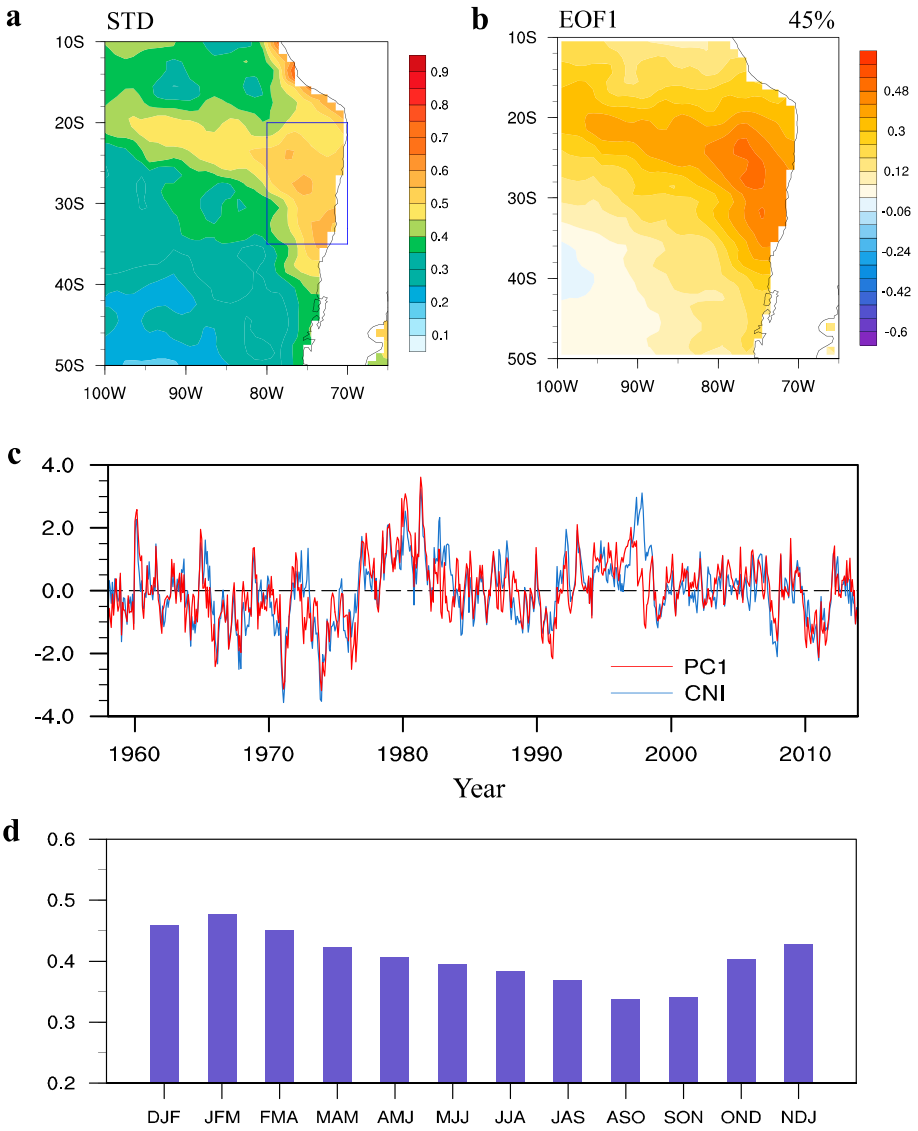

Figure 1. The spatiotemporal characteristics of Chile Niño/Niña mode. (a) Standard deviation and (b) first empirical orthogonal function (EOF) mode of monthly SST anomalies during 1958–2013 derived from the residual HadISST data after linearly removing the ENSO signal. The blue box in (a) denotes the region for Chile Niño/Niña index (CNI). The percentage of total variance explained by the EOF1 reaches 45%. (c) Normalized time series of EOF1 (red) and CNI (blue). (d) The seasonally stratified standard deviation of the CNI.

ocean with negative geopotential height anomalies in the lower troposphere (Figure S7). This strengthens the land-sea contrast in near-surface pressure anomaly, reinforces the anomalies of southward alongshore winds in turn and thus further weakens the coastal upwelling. As a result, the initial warm SST anomalies grow. To illustrate more clearly the air-sea coupled processes over the coastal Chile Niño/Niña region, Figure 3 shows the lead-lag correlations of JFM CNI with the alongshore wind index and coastal upwelling index (see section 2.2). The anomalies in SST evolve synchronously with the alongshore surface winds and coastal upwelling anomalies, reaching the peak phase in JFM. The coevolution of these variables demonstrates the coastal Bjerknes feedback plays an essential role in driving the development of Chile Niño/Niña.

In addition to the dynamical coastal Bjerknes feedback, anomalous surface heating also contributes to the evolution of Chile Niño. As illustrated in Figure S8, anomalous surface warming is observed over the Chile Niño region during the developing phase. It should be noted that this anomalous surface heating is associated with changes in both the net surface heat flux into the ocean and MLD (equation (2)). Because the surface wind anomalies are against the climatology, the MLD is anomalously shoaled due to the

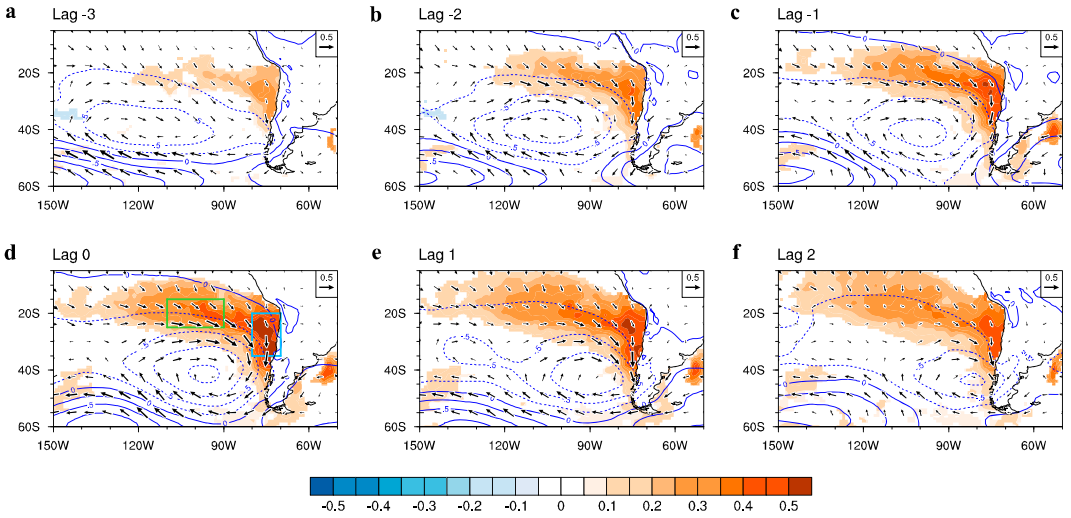

Figure 2. Atmospheric circulation and SST anomalies associated with Chile Niño. (a–f) Lead-lag regressions of 3-month running averaged SST (°C; shading), sea level pressure (hPa; contours) and 10-m winds (m s^{-1}; vectors) onto the normalized JFM CNI for the period 1958–2013. Negative (positive) lags indicate the months that the JFM CNI lags (leads). Shown are only the regressed SST anomalies that are significant at the 95% confidence level (based on a two-tailed Student's *t* test). The domains used to calculate mixed-layer heat balance for the nearshore (blue box; 80°–70°W, 35°–20°S) and offshore (green box; 110°–90°W, 25°–15°S) Chile Niño/Niña regions are indicated in (d).

weakened surface wind speed, and significant negative correlations between JFM CNI and mixed-layer depth index (see section 2.2) are thus observed (blue line in Figure 3). Therefore, during the developing phase of Chile Niño, the anomalously thin MLD amplifies the warming effect of the positive net surface heat flux (Figure S9).

3.3. Mixed-Layer Heat Balance Analyses for Chile Niño/Niña Evolution

To measure the relative importance of various processes that contribute to the Chile Niño/Niña evolution, we analyzed the mixed-layer heat balance in detail over the nearshore region (the blue box in Figure 2d). As shown in Figure 4, during the developing phase, the tendency of SST is highly positive and reaches a maximum two months before the peak (black solid line). The ocean vertical processes (red dashed line) and surface heating (orange dashed line) are two major contributors to the positive SST tendency. The warming effect of the ocean vertical processes is largely related to surface wind reduction; the anomalous southward alongshore winds weaken the coastal upwelling, and the decreased climatological equatorward surface winds weaken the entrainment of the subsurface cold water by the wind stirring, thus leading to the warming of SST.

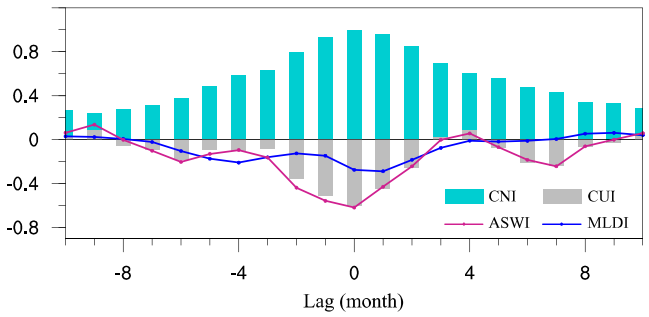

Figure 3. Ocean-atmosphere coupled processes linked to Chile Niño. Lead-lag correlation coefficients between JFM CNI and 3-month running mean CNI (green filled bar), alongshore wind index (ASWI; red line), and coastal upwelling index (CUI; gray filled bar) for the period 1958–2013. Similar lead-lag correlation between JFM CNI and the mixed-layer depth index (MLDI; blue line) during 1958–2010 is also plotted. Negative (positive) numbers in *X* axis indicate the months that JFM CNI lags (leads). Correlation coefficients above (below) 0.26 (−0.26) are significant at the 95% confidence level.

Figure 4b further decomposes the contribution of net surface heat flux into four components. We find surface warming is caused by the surface shortwave radiation (red dashed line) and sensible heat flux (orange dashed line), whereas contributions of latent heat flux have cooling effects oppositely. Owing to strong subsidence of air-flow near the eastern edge of the subtropical high, the ocean there is covered generally by low-level stratus clouds that have cooling effects on the surface by reflecting back the shortwave radiation (Klein et al., 1995; Klein & Hartmann, 1993). Previous studies suggested the SST-low stratus clouds feedback plays an important role in climate variability over the eastern subtropical oceans (Clement et al., 2009; Philander et al., 1996). To examine possible roles of the above process, the lead-lag regressed patterns of surface net shortwave radiation and low cloud cover are shown in Figure S10. Accompanying the initial warm SST anomalies, the amount of low cloud cover over the nearshore Chile Niño region is decreased significantly,

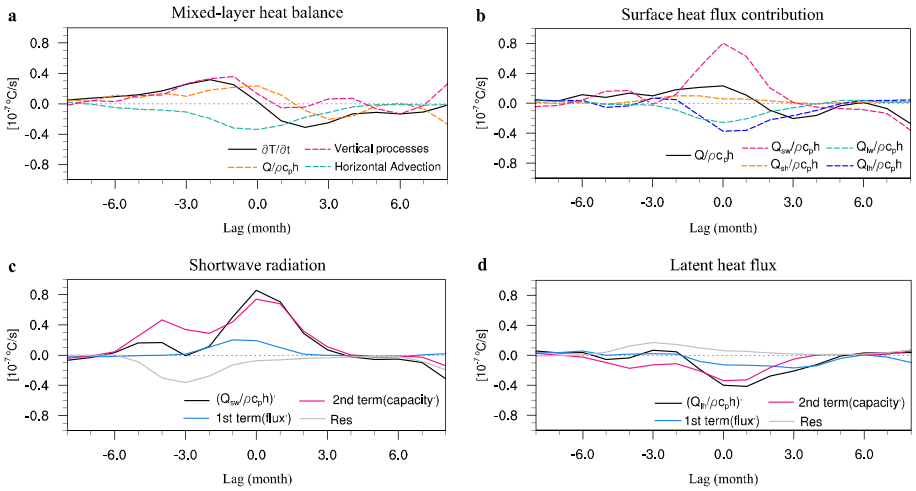

Figure 4. Mixed-layer heat budget governing the Chile Niño evolution. (a) Mixed-layer heat balance and (b) surface heat flux contribution averaged over the nearshore box of Chile Niño region during 1958–2010, shown as lead-lag regressions onto the normalized JFM CNI. In (a), regressed anomalies of mixed-layer temperature tendency (black solid line) and its three contributors: warming/cooling by net surface heat flux (orange dashed line), ocean vertical processes (red dashed line), and horizontal advection (green dashed line). In (b), regressed anomaly of total surface heat flux contribution (black solid line) and anomalous contributions from the shortwave radiation (red dashed line), longwave radiation (green dashed line), latent heat flux (blue dashed line), and the sensible heat flux (orange dashed line). (c) Lead-lag regression of terms in equation (2) onto the normalized JFM CNI for the shortwave radiation. The total contribution anomaly (black line), the first term (blue line, flux anomaly effect), the second term (red line, capacity anomaly effect), and the residual (gray line) on the right-hand side of equation (2) are shown. (d) As in (c), but for the latent heat flux.

which leads to increased downward shortwave radiation and thus reinforces the warm SST anomalies. The SST-stratus clouds-shortwave radiation positive feedback certainly exists and is responsible for the positive flux anomaly of shortwave radiation (blue line in Figure 4c). Moreover, the residual representing nonlinear terms have negative contribution during the developing phase (gray line in Figure 4c). However, as seen clearly in Figure 4c, the net anomalous contribution of shortwave radiation comes from the effect of the heat capacity variation; the thinner mixed layer is more effectively warmed even by the climatological downward shortwave radiation (red line in Figure 4c). Comparing those three contributors, the net mixed-layer warming by shortwave radiation is mostly due to the thinner MLD, which reduces the ocean heat capacity. Though the shoaled MLD plays an opposite role, the sensible heat flux still has a weak warming effect due to more dominant flux anomaly effect; the reduction in surface wind speed leads to anomalous downward sensible heat flux (Figures S11 and S12). In addition, because of the anomalously thin MLD and increased ocean-atmosphere specific humidity difference, the cooling effect of latent heat flux is even enhanced despite the reduced surface wind speed (Figures 4d and S13), suggesting that the wind-evaporation-SST feedback (Lin et al., 2008; Xie & Philander, 1994) does not operate at least in the region of the present interest.

The Chile Niño reaches the peak in austral summer when the climatological MLD is the shallowest. After the peak phase, accompanying the seasonal deepening of climatological MLD ($\overline{h}$ in equation (2)), the net surface warming of the mixed-layer by shortwave radiation is reduced (Figures 4c and S5). As such, the positive SST anomalies related to Chile Niño gradually decay. Additionally, the ocean horizontal advection also cools SST anomalies. Accompanying the weakening of climatological equatorward alongshore winds, the sea surface height is anomalously raised offshore compared to the coast. The positive anomalies in sea surface height corresponds to anomalous northward ocean currents along the Chilean coast, which increase the equatorward advection of cold water by the Humboldt Current, thus damping the warm SST anomalies further. (green dashed line in Figures 4a and S14).

4. Summary and Discussion

The devastating Ningaloo Niño event that occurred in the summer of 2011 generated among the climate research community keen renewed interests in marine heat waves (extreme events including cold waves)

associated with air-sea interactions along the eastern boundaries of major subtropical oceans. In addition to the well-known Benguela Niño/Niña off the west coast of southern Africa, two more coastal air-sea coupled phenomena (i.e., coastal Niño/Niña) have been found to exist near the eastern boundary of subtropical oceans since the discovery of Ningaloo Niño/Niña. Those are California Niño/Niña in the North Pacific and Dakar Niño/Niña in the North Atlantic (Oettli et al., 2016; Yuan & Yamagata, 2014). However, it is not reported near the eastern boundary in the South Pacific. In the present study, we have discovered a new coupled climate mode off Chile for the first time by carefully removing the ENSO interference and have named the phenomenon Chile Niño/Niña for easy future reference.

The coastal SST anomalies related to Chile Niño/Niña are accompanied by the synchronous evolution of alongshore surface winds, coastal upwelling, and the MLD, demonstrating the essential role of regional air-sea coupled dynamics. The mixed-layer heat balance analyses show the anomalous coastal SST warming (cooling) is due to the contribution of both the suppressed (enhanced) ocean vertical processes and increased (decreased) surface shortwave radiation heating effects through anomalously thin (thick) MLD. This regional climate mode shows prominent seasonal phase-locking nature due to the annual cycle of climatological MLD, which is the shallowest in austral summer. The above analyses of Chile Niño/Niña evolution are for the nearshore box (blue rectangle in Figure 2d). However, the holistic pattern of Chile Niño/Niña extends from the nearshore region to the open ocean, and the SST anomalies in the offshore box (green rectangle in Figure 2d; 110°–90°W, 25°–15°S) could be generated by a different mechanism and needs to be checked. Mixed-layer heat budget analyses over the offshore box suggest the generation and decay of offshore SST anomalies are dominantly contributed by surface heating/cooling, while vertical processes help decay the warm SST anomalies (Figure S15). During the developing phase, the positive (negative) SST anomalies in the offshore box are induced by increased (decreased) shortwave radiation contribution due to anomalously thinned (thickened) MLD. Again, the wind-evaporation-SST feedback mechanism does not operate at all, suggesting quantitative reexamination in the evolution of other climate modes.

For simplicity, the linear correlations/regressions are employed in the present work to reveal the general life cycle of Chile Niño; the evolution of Chile Niña is just a mirror image of that for Chile Niño. However, some asymmetric nature may exist in reality between Chile Niño and Chile Niña. As shown in Figures S16 and S17 prepared by the composite analysis based on the seasonally phase-locked nature, Chile Niña seems to extend more westward than Chile Niño, but decay more quickly as indicated by changes of surface wind anomalies.

The Chile Niño/Niña is found to develop and decay under regional processes. However, how this coastal climate mode is triggered remains unknown. Our preliminary results suggest the anomalous cyclone (anticyclone) of the South Pacific High which triggers Chile Niño (Niña) seems to be associated with a teleconnection pattern emanating from the South Pacific Convergence Zone, where the convection is anomalously decreased (Figure S18). Therefore, the trigger of Chile Niño/Niña may have a relation with the variability of the South Pacific High and the South Pacific Convergence Zone, and this certainly deserves further detailed analyses.

This study reveals the existence and generation mechanism of new Chile Niño/Niña mode based on relatively coarse ocean data sets, which may be unable to identify the intricate ocean-atmosphere structure. However, we believe that to identify the concrete climate mode is the first step to improve the climate models as well as to understand the phenomenon in more detail. Owning to noticeable impacts of coastal Niño/Niña events on marine ecology and regional climate, Chile Niño/Niña may has great implications for regional fish production and blue economy just like its counterparts in other regions. By using an atmosphere-ocean coupled general circulation model, some of the Ningaloo Niño/Niña events in austral summer are found predictable two seasons in advance (Doi et al., 2013). However, most coastal Niño/Niña regions are suffering from warm SST biases in all climate models (Prospectus for CLIVAR Research Focus on Eastern Boundary Upwelling Systems, 2018; Wang et al., 2014). Therefore, efforts to fix model biases and develop a seasonal prediction system focusing on the coastal Niño/Niña will benefit the livelihood of people just like those efforts to predict the basin-wide climate modes like ENSO and IOD (Luo et al., 2005).

Acknowledgments
We appreciate the reviewers for their helpful comments. This work is sponsored by The Startup Foundation for Introducing Talent of NUIST (1091011901003). Jing-Jia Luo is supported by The Startup Foundation for Introducing Talent of NUIST. The HadISST was downloaded from https://www.metoffice.gov.uk/hadobs/ website. The JRA-55 is provided by research data archive at NCAR and is available at https://rda.ucar.edu/datasets/ds628.1/ website. The SODA data set was downloaded from http://www.soda.umd.edu/ website. The GODAS data is obtained from https://www.esrl.noaa.gov/psd/data/gridded/data.godas.html/ website.

References

Barrett, B. S., Campos, D. A., Vicencio Veloso, J., & Rondanelli, R. (2016). Extreme temperature and precipitation events in March 2015 in central and northern Chile. *Journal of Geophysical Research: Atmospheres*, *121*, 4563–4580. https://doi.org/10.1002/2016JD024835

Behringer, D. W., & Xue, Y. (2004). Evaluation of the global ocean data assimilation system at NCEP: The Pacific Ocean. Eighth Symposium on Integrated Observing and Assimilation Systems for Atmosphere, Oceans, and Land Surface, AMS 84th Annual Meeting, Washington State Convention and Trade Center, Seattle, Washington. 11-15.

Binet, D., Gobert, B., & Maloueki, L. (2001). El Niño-like warm events in the Eastern Atlantic (6°N, 20°S) and fish availability from Congo to Angola (1964–1999). *Aquatic Living Resources*, *14*, 99–113. https://doi.org/10.1016/S0990-7440(01)01105-6

Bjerknes, J. (1969). Atmospheric teleconnections from the equatorial Pacific. *Monthly Weather Review*, *97*(3), 163–172. https://doi.org/10.1175/1520-0493(1969)097<0163:ATFTEP>2.3.CO;2

Capone, D. G., & Hutchins, D. A. (2013). Microbial biogeochemistry of coastal upwelling regimes in a changing ocean. *Nature Geoscience*, *6*(9), 711–717. https://doi.org/10.1038/ngeo1916

Carton, J. A., & Giese, S. G. (2008). A reanalysis of ocean climate using Simple Ocean Data Assimilation (SODA). *Monthly Weather Review*, *136*(8), 2999–3017. https://doi.org/10.1175/2007MWR1978.1

Castelao, R. M., & Barth, J. A. (2006). Upwelling around Cabo Frio, Brazil: The importance of wind stress curl. *Geophysical Research Letters*, *33*, L03602. https://doi.org/10.1029/2005GL025182

Clement, A. C., Burgman, R., & Norris, J. R. (2009). Observational and model evidence for positive low-level cloud feedback. *Science*, *325*(5939), 460–464. https://doi.org/10.1126/science.1171255

de Boyer Montégut, C., Madec, G., Fischer, A. S., Lazar, A., & Ludicone, D. (2004). Mixed layer depth over the global ocean: An examination of profile data and a profile-based climatology. *Journal of Geophysical Research*, *109*, C12003. https://doi.org/10.1029/2004JC002378

Depczynski, M., Gilmour, J. P., Ridgway, T., Barnes, H., Heyward, A. J., Holmes, T. H., et al. (2013). Bleaching, coral mortality and subsequent survivorship on a West Australian fringing reef. *Coral Reefs*, *32*(1), 233–238. https://doi.org/10.1007/s00338-012-0974-0

Doi, T., Behera, S. K., & Yamagata, T. (2013). Predictability of the Ningaloo Niño. *Scientific Reports*, *3*(1), 2892. https://doi.org/10.1038/srep02892

Durazo, R., & Baumgartner, T. R. (2002). Evolution of oceanographic conditions off Baja California: 1997–1999. *Progress in Oceanography*, *54*(1-4), 7–31. https://doi.org/10.1016/S0079-6611(02)00041-1

Feng, M., McPhaden, M. J., Xie, S.-P., & Hafner, J. (2013). La Niña forces unprecedented Leeuwin Current warming in 2011. *Scientific Reports*, *3*(1), 1277. https://doi.org/10.1038/srep01277

Fennel, W., Junker, T., Schmidt, M., & Mohrholz, V. (2012). Response of the Benguela upwelling systems to spatial variations in the wind stress. *Continental Shelf Research*, *45*, 65–77. https://doi.org/10.1016/j.csr.2012.06.004

Greatbatch, R. J. (1985). On the role played by upwelling of water in lowering sea surface temperatures during the passage of a storm. *Journal of Geophysical Research*, *90*, 11,751–11,755.

Hu, Z.-Z., Huang, B., Zhu, J., Kumar, A., & McPhaden, M. J. (2019). On the variety of coastal El Niño events. *Climate Dynamics*, *52*(12), 7537–7552. https://doi.org/10.1007/s00382-018-4290-4

Kataoka, T., Tozuka, T., Behera, S., & Yamagata, T. (2014). On the Ningaloo Niño/Niña. *Climate Dynamics*, *43*(5-6), 1463–1482. https://doi.org/10.1007/s00382-013-1961-z

Kataoka, T., Tozuka, T., & Yamagata, T. (2017). Generation and decay mechanisms of Ningaloo Niño/Niña. *Journal of Geophysical Research: Oceans*, *122*, 8913–8932. https://doi.org/10.1002/2017JC012966

Klein, S. A., & Hartmann, D. L. (1993). The seasonal cycle of low stratiform clouds. *Journal of Climate*, *6*(8), 1587–1606. https://doi.org/10.1175/1520-0442(1993)006<1587:TSCOLS>2.0.CO;2

Klein, S. A., Hartmann, D. L., & Norris, J. R. (1995). On the relationships among low cloud structure, sea surface temperature, and atmospheric circulation in the summertime northeast Pacific. *Journal of Climate*, *8*(5), 1140–1155. https://doi.org/10.1175/1520-0442(1995)008%3C1140:OTRALC%3E2.0.CO;2

Kobayashi, S., Ota, Y., Harada, Y., Ebita, A., Moriya, M., Onoda, H., et al. (2015). The JRA-55 reanalysis: General specifications and basic characteristics. *Journal of the Meteorological Society of Japan*, *93*(1), 5–48. https://doi.org/10.2151/jmsj.2015-001

Lin, J.-L., Han, W., & Lin, X. (2008). Observational analysis of the wind-evaporation-SST feedback over the tropical Pacific Ocean. *Atmospheric Science Letters*, *9*, 231–236. https://doi.org/10.1002/asl.195

Lübbecke, J. F., Böning, C. W., Keenlyside, N. S., & Xie, S.-P. (2010). On the connection between Benguela and equatorial Atlantic Niños and the role of the South Atlantic Anticyclone. *Journal of Geophysical Research*, *115*, C09015. https://doi.org/10.1029/2009JC005964

Lübbecke, J. F., Rudloff, D., & Stramma, L. (2019). Stand-alone eastern Pacific Coastal Warming events. *Geophysical Research Letters*, *46*, 12,360–12,367. https://doi.org/10.1029/2019GL084479

Luo, J. -J., Masson, S., Behera, S., Shingu, S., & Yamagata, T. (2005). Seasonal climate predictability in a coupled OAGCM using a different approach for ensemble forecasts. *Journal of Climate*, *18*(21), 4474–4497. https://doi.org/10.1175/JCLI3526.1

Morioka, Y., Tozuka, T., Masson, S., Terray, P., Luo, J.-J., & Yamagata, T. (2012). Subtropical dipole modes simulated in a coupled general circulation model. *Journal of Climate*, *25*(12), 4029–4047. https://doi.org/10.1175/JCLI-D-11-00396.1

Morioka, Y., Tozuka, T., & Yamagata, T. (2010). Climate variability in the southern Indian Ocean as revealed by self-organizing maps. *Climate Dynamics*, *35*(6), 1059–1072. https://doi.org/10.1007/s00382-010-0843-x

Morioka, Y., Tozuka, T., & Yamagata, T. (2011). On the growth and decay of the subtropical dipole mode in the South Atlantic. *Journal of Climate*, *24*, 5538–5554. https://doi.org/10.1175/2011JCLI4010.1

Oettli, P., Morioka, Y., & Yamagata, T. (2016). A regional climate mode discovered in the North Atlantic: Dakar Niño/Niña. *Scientific Reports*, *6*(1), 18782. https://doi.org/10.1038/srep18782

Pearce, A. F., & Feng, M. (2013). The rise and fall of the "marine heat wave" off Western Australia during the summer of 2010/2011. *Journal of Marine Systems*, *111–112*, 139–156. https://doi.org/10.1016/j.jmarsys.2012.10.009

Philander, S. G. H. (1990). *El Niño, La Niña, and the Southern Oscillation*. Cambridge, MA: Academic Press.

Philander, S. G. H., Gu, D., Lambert, G., Li, T., Halpern, D., Lau, N. C., & Pacanowski, R. C. (1996). Why the ITCZ is mostly north of the equator. *Journal of Climate*, *9*(12), 2958–2972. https://doi.org/10.1175/1520-0442(1996)009<2958:WTIIMN>2.0.CO;2

Philander, S. G. H., Yamagata, T., & Pacanowski, R. C. (1984). Unstable air-sea interactions in the tropics. *Journal of the Atmospheric Sciences*, *41*(4), 604–613. https://doi.org/10.1175/1520-0469(1984)041<0604:UASIIT>2.0.CO;2

Pickett, M. H., & Paduan, J. D. (2003). Ekman transport and pumping in the California Current based on the U.S. Navy's high-resolution atmospheric model (COAMPS). *Journal of Geophysical Research*, *108*(C10), 3327. https://doi.org/10.1029/2003JC001902

Prospectus for CLIVAR Research Focus on Eastern Boundary Upwelling Systems (RF-EBUS) (2018). Retrieved from http://www.clivar.org/sites/default/files/Revised-EBUS-Prospectus_July2018.pdf

Rayner, N., Parker, D. E., Horton, E., Folland, C., Alexander, L., Rowell, D., et al. (2003). Global analyses of sea surface temperature, sea ice, and night marine air temperature since the late nineteenth century. *Journal of Geophysical Research*, *108*(D14), 4407. https://doi.org/10.1029/2002JD002670

Saji, N. H., Goswami, B. N., Vinayachandran, P. N., & Yamagata, T. (1999). A dipole mode in the tropical Indian Ocean. *Nature*, *401*(6751), 360–363. https://doi.org/10.1038/43854

Santos, F., deCastro, M., Gomez-Gesteria, M., & Alvarez, I. (2012). Differences in coastal and oceanic SST warming rates along the Canary upwelling ecosystem from 1982 to 2010. *Continental Shelf Research*, *47*, 1–6. https://doi.org/10.1016/j.csr.2012.07.023

Shannon, L. V., Boyd, A. J., Brundrit, G. B., & Taunton-Clark, J. (1986). On the existence of an El Niño-type phenomenon in the Benguela system. *Journal of Marine Research*, *44*(3), 495–520. https://doi.org/10.1357/002224086788403105

Simpson, J. J. (1983). Large-scale thermal anomalies in the California Current during the 1982–1983 El Niño. *Geophysical Research Letters*, *10*, 937–940. https://doi.org/10.1029/GL010i010p00937

Takahashi, K., & Martínez, A. G. (2019). The very strong coastal El Niño in 1925 in the far-eastern Pacific. *Climate Dynamics*, *52*(12), 7389–7415. https://doi.org/10.1007/s00382-017-3702-1

Tozuka, T., Kataoka, T., & Yamagata, T. (2014). Locally and remotely forced atmospheric circulation anomalies of Ningaloo Niño/Niña. *Climate Dynamics*, *43*(7-8), 2197–2205. https://doi.org/10.1007/s00382-013-2044-x

Wang, C., Zhang, L., Lee, S. K., Wu, L., & Mechoso, C. R. (2014). A global perspective on CMIP5 climate model biases. *Nature Climate Change*, *4*(3), 201–205. https://doi.org/10.1038/nclimate2118

Webster, P. J., Moore, A. M., Loschnigg, J. P., & Leben, R. R. (1999). Coupled ocean-atmosphere dynamics in the Indian Ocean during 1997–98. *Nature*, *401*(6751), 356–360. https://doi.org/10.1038/43848

Wernberg, T., Smale, D. A., Tuya, F., Thomsen, M. S., Langlois, T. J., de Bettignies, T., et al. (2013). An extreme climatic event alters marine ecosystem structure in a global biodiversity hotspot. *Nature Climate Change*, *3*(1), 78–82. https://doi.org/10.1038/nclimate1627

Wilcox, A. C., Escauriaza, C., Agredano, R., Mignot, E., Zuazo, V., Otárola, S., et al. (2016). An integrated analysis of the March 2015 Atacama floods. *Geophysical Research Letters*, *43*, 8035–8043. https://doi.org/10.1002/2016GL069751

Xie, S. P., & Philander, S. G. H. (1994). A coupled ocean-atmosphere model of relevance to the ITCZ in the eastern Pacific. *Tellus A*, *46*(4), 340–350. https://doi.org/10.3402/tellusa.v46i4.15484

Yoshida, K. (1959). A theory of the Cromwell current and of the equatorial upwelling—An interpretation in a similarity to a coastal circulation. *Journal of the Oceanographical Society of Japan*, *15*(4), 159–170. https://doi.org/10.5928/kaiyou1942.15.159

Yuan, C., & Yamagata, T. (2014). California Niño/Niña. *Scientific Reports*, *4*(1), 4801. https://doi.org/10.1038/srep04801

Zebiak, S. E. (1993). Air-sea interaction in the equatorial Atlantic region. *Journal of Climate*, *6*(8), 1567–1586. https://doi.org/10.1175/1520-0442(1993)006<1567:AIITEA>2.0.CO;2